A STUDY OF DIABATIC HEATING EFFECTS ON THE DEVELOPMENT OF PRESSURE WAVES

ELIZABETH M. BARRETT

A STUDY OF DIABATIC HEATING EFFECTS ON THE DEVELOPMENT OF PRESSURE WAVES

* * * * *

Elizabeth M. Barrett

A STUDY OF DIABATIC HEATING EFFECTS ON THE DEVELOPMENT OF PRESSURE WAVES

by

Elizabeth M. Barrett
Lieutenant Commander, United States Navy

Submitted in partial fulfillment of
the requirements for the degree of

MASTER OF SCIENCE
IN
METEOROLOGY

United States Naval Postgraduate School
Monterey, California

1 9 6 5

A STUDY OF DIABATIC HEATING EFFECTS ON THE DEVELOPMENT OF PRESSURE WAVES

by

Elizabeth M. Barrett

This work is accepted as fulfilling
the thesis requirements for the degree of
MASTER OF SCIENCE
IN
METEOROLOGY
from the
United States Naval Postgraduate School

ABSTRACT

A baroclinic model programmed for numerical solution is used to investigate the effects of diabatic heating on the development of pressure waves for periods up to 24 hours. Several forms of the model are studied with results being obtained for various wavelengths. The results lead to some meteorological improbabilities; however, the relative development of the pressure wave appears valid for short time periods.

The writer wishes to express her appreciation to Professor George Haltiner of the U. S. Naval Postgraduate School for his assistance and guidance in this investigation. Appreciation is also expressed to LT Jack Nourie, USN, for his assistance in preparing diagrams and compiling data.

TABLE OF CONTENTS

LIST OF SYMBOLS

Variables and Constants - Roman Alphabet

A - D	amplitudes of various sine and cosine functions
C_R	Rossby wave speed, $= U - \beta/k^2$
E - H	shorthand equivalent of various equations as designated in text, (appear with or without primes)
f	the Coriolis parameter, $2\Omega \sin\varphi$
f_o	an average value of the Coriolis parameter
g	acceleration of gravity
i	unit vector in X direction
k	unit vector in Z direction
k	wave number, $2\pi/L$
L	wave length
p	atmospheric pressure
Q	heating term
R_z	amplitude of the pressure wave
t	time
U	mean zonal flow in X direction
u	component of perturbation velocity in X direction
V	horizontal velocity vector
v	component of velocity in Y direction
x	coordinate toward east
y	coordinate toward north
z	height of isobaric surface

Variables and Constants - Greek Alphabet

α	coefficient of certain terms, $2 + 46\left(\frac{k \Delta p}{f_o}\right)^2$
β	variation of the Coriolis parameter, $\partial f / \partial y$
ζ	vertical component of relative vorticity, $= \frac{1}{f_o} \nabla^2 \phi$
δ	phase angle
θ	potential temperature
σ	stability factor, $= \frac{1}{\theta} \frac{\partial \phi}{\partial P} \frac{\partial \theta}{\partial P}$
ϕ	geopotential, gz
φ	geographical latitude
ω	total derivative of pressure with respect to time
Ω	the angular speed of the earth's rotation
τ	positive tolerance

Subscripts and Superscripts

i	vertical index denoting a pressure level
n	index denoting the nth estimate of a quantity

Operators

∇	two dimensional del operator on a constant pressure surface
∇^2	Laplacian operator
Δ	finite difference operator with respect to p and t
$\lvert ( ) \rvert$	absolute value of a quantity

1. Introduction

Most numerical prediction methods for obtaining prognostic charts of the pressure field neglect diabatic heating effects under the assumption that their influence is negligible for short period prognosis.

Under certain circumstances, however, the exchange of sensible heat between an air mass and the underlying surface may be considerable. It is therefore the purpose of this paper to investigate the effects of such diabatic exchange on the development of pressure waves for periods up to 24 hours using a numerical model.

2. The Model

The model with which the aforementioned heating effects were studied was developed from the geostrophic relationship, the vorticity equation, and the thermodynamic equation,

$$V = \frac{k}{f_0} \times \nabla \phi, \tag{1}$$

$$\frac{\partial \zeta}{\partial t} + V \cdot \nabla (f + \zeta) = f_0 \frac{\partial \omega}{\partial p}, \tag{2}$$

$$\frac{\partial^2 \phi}{\partial p \partial t} + V \cdot \nabla \frac{\partial \phi}{\partial p} + \sigma \omega = - \frac{Q}{p}. \tag{3}$$

The dependent variables are expressed as the sum of a base state plus perturbation quantity (indicated by a prime),

$$\phi = \bar{\phi}(p, y) + \phi'(x, y, p, t), \tag{4}$$

$$V = u(p) i + V'(x, y, p, t), \tag{5}$$

$$\omega = \omega'(x, y, p, t), \tag{6}$$

$$Q = \bar{Q}(p) + Q'(p) \quad \text{with } \bar{Q}(p) = 0, \tag{7}$$

$$\zeta = \bar{\zeta} + \zeta'. \tag{8}$$

Equations (2) and (3) are then linearized by the usual method of assuming that they are satisfied by the basic quantities alone and by the total quantities (sum of the basic plus perturbation). Subtracting the equations for the basic flow from the total equations and neglecting products of perturbation quantities yields

$$\nabla^2 \frac{\partial \phi'}{\partial t} + u \nabla^2 \frac{\partial \phi'}{\partial x} + \beta \frac{\partial \phi'}{\partial x} = f_0^2 \frac{\partial \omega'}{\partial p}, \tag{9}$$

$$\frac{\partial^2 \phi'}{\partial p \partial t} + u \frac{\partial^2 \phi'}{\partial x \partial p} + v \frac{\partial^2 \phi'}{\partial y \partial p} + \sigma \omega' = - \frac{Q'}{p}. \tag{10}$$

Equation (10) is further modified by substituting for the third term

$$v \frac{\partial^2 \bar{\phi}}{\partial y \partial p} = - \frac{\partial \phi'}{\partial x} \frac{\alpha u}{\alpha p} \tag{11}$$

yielding,

$$\frac{\partial^2 \phi'}{\partial p \partial t} + u \frac{\partial^2 \phi'}{\partial x \partial p} - \frac{\partial \phi'}{\partial x} \frac{\alpha u}{\alpha p} + \sigma \omega' = - \frac{Q'}{p}. \tag{12}$$

A diagnostic equation for the vertical velocity is obtained by differentiating (9) with respect to p, taking the Laplacian of (12), and subtracting, resulting in

$$2 \frac{\alpha u}{\alpha p} \nabla^2 \frac{\partial \phi'}{\partial x} + \beta \frac{\partial^2 \phi'}{\partial p \partial x} = f_0^2 \frac{\partial^2 \omega'}{\partial p^2} + \sigma \nabla^2 \omega' + \nabla^2 \frac{Q'}{p}. \tag{13}$$

Solutions are now assumed to be of the form

$$z' = \frac{\phi'}{g} = A(p,t) \sin kx + B(p,t) \cos kx, \tag{14}$$

$$\omega' = C(p,t) \sin kx + D(p,t) \cos kx, \tag{15}$$

$$Q' = Q_1 (\sin kx + \delta_1) + Q_2 (\cos kx + \delta_2). \tag{16}$$

Next equations (14) through (16) are substituted into equations (9) and (13), and the coefficients of sinkx and cos kx equated giving

$$\frac{\partial A}{\partial t} = k C_R B - \frac{f_0^2}{g k^2} \frac{\partial C}{\partial p}, \tag{17}$$

$$\frac{\partial B}{\partial t} = - k C_R A - \frac{f_0^2}{g k^2} \frac{\partial D}{\partial p}, \tag{18}$$

$$\frac{\partial^2 C}{\partial p^2} - \frac{\sigma k^2 C}{f_0^2} = 2 g B \frac{k^3}{f_0^2} \frac{\alpha u}{\alpha p} - \frac{\beta g}{f_0^2} \frac{k \partial B}{\partial p} - \frac{k^2}{f_0^2} (Q_2 \sin \delta_2 - Q_1 \cos \delta_1), \tag{19}$$

$$\frac{\partial^2 D}{\partial p^2} - \frac{\sigma k^2 D}{f_0^2} = - 2 g A \frac{k^3}{f_0^2} \frac{\alpha u}{\alpha p} + \frac{\beta g k}{f_0^2} \frac{\partial A}{\partial p} + \frac{k^2}{f_0^2} (Q_2 \cos \delta_2 + Q_1 \sin \delta_1). \tag{20}$$

Equations (17) through (20) are then solved numerically as an initial value problem as outlined by Rosenthal [1] . Given initial values of A and B, equations (19) and (20) are solved to obtain C and D. These in turn are substituted into (17) and (18) to obtain prognostic values for A and B. The computational cycle is continued for the desired time interval.

3. Procedures

Using finite differencing, the diagnostic equations, (19) and (20), can be approximated at the odd levels as

$$C_{i+2} - \alpha C_i + C_{i-2} = 4K\Delta P\left(\frac{k}{f_0}\right)^2 g\,(U_{i+1} - U_{i-1})B_i - \frac{2\beta k \Delta P g}{f_0^2}(B_{i+1} - B_{i-1}) \qquad (19a)$$
$$- 4\left(\frac{k}{f_0}\right)^2 \frac{1}{P}(Q_2 \sin\delta_2 - Q_1 \cos\delta_1) \equiv -H_i ,$$

$$D_{i+2} - \alpha D_i + D_{i-2} = -4K\Delta P\left(\frac{k}{f_0}\right)^2 g\,(U_{i+1} - U_{i-1})A_i + \frac{2\beta k \Delta P}{f_0^2}(A_{i+1} - A_{i-1})$$
$$+ 4\left(\frac{k}{f_0}\right)^2 \frac{1}{P}(Q_2 \cos\delta_2 + Q_1 \sin\delta_1) \equiv -H_i' . \qquad (20a)$$

$$i = 3,5,\ldots..19$$

At the even levels C and D are obtained by simple averaging,

$$C_i = \frac{C_{i+1} + C_{i-1}}{2}, \quad D_i = \frac{D_{i+1} + D_{i-1}}{2} . \qquad (21)$$

$$i = 2,4,\ldots..20$$

Boundary conditions are that C and D at the top and bottom levels are zero, implying a vanishing vertical velocity there.

The prognostic equations, (17) and (18) are approximated at the even levels by

$$\frac{\partial A_i}{\partial t} = k C_R B_i - \left(\frac{f_0}{k}\right)^2 \frac{1}{g}\left(\frac{C_{i+1} - C_{i-1}}{2\Delta P}\right) \equiv G_i , \qquad (17a)$$

$$\frac{\partial B_i}{\partial t} = -k C_R A_i - \left(\frac{f_0}{k}\right)^2 \frac{1}{g}\left(\frac{D_{i+1} - D_{i-1}}{2\Delta P}\right) \equiv G_i' . \qquad (18a)$$

$$i = 2,4,\ldots..20$$

At the odd levels, A and B are obtained by averaging,

$$A_i = \frac{A_{i+1} + A_{i-1}}{2}, \quad B_i = \frac{B_{i+1} + B_{i-1}}{2} . \qquad (22)$$

$$i = 3,5,\ldots..19$$

A vertical increment of 50 mb is used, affording considerable vertical resolution. This yields a 21 point vertical grid with 0 mb as level 1 and 1000 mb as level 21, as shown in figure 1.

Figure 1 - Finite Difference Grid

Grid-point index	Grid-point pressure	Equation applied
1	0	
2	50	vorticity
3	100	omega
4	150	vorticity
5	200	omega
6	250	vorticity
7	300	omega
8	350	vorticity
9	400	omega
10	450	vorticity
11	500	omega
12	550	vorticity
13	600	omega
14	650	vorticity
15	700	omega
16	750	vorticity
17	800	omega
18	850	vorticity
19	900	omega
20	950	vorticity
21	1000	

The values of C and D are obtained by a simple relaxation scheme as follows:

$$E_i = \frac{1}{\alpha_i - E_{i-2}} \quad , \tag{23}$$

$$F_i = \frac{H_i + F_{i-2}}{\alpha_i - E_{i-2}} \quad , \tag{24}$$

$$F_i' = \frac{H_i' + F_{i-2}'}{\alpha_i - E_{i-2}} \quad , \tag{25}$$

$i = 3,5,.....19$, and $E_1, F_1, F_1' \equiv 0$, then

$$C_i = E_i C_{i+2} + F_i \quad , \tag{26}$$

$$D_i = E_i D_{i+2} + F_i' \qquad (27)$$

$$i = 19, 17, \cdots 3$$

Equations (17a) and (18a) are solved by an iteration technique as follows,

$$A_i^{(n+1)}(t+\Delta t) = A_i(t) + \frac{\Delta t}{2}\left[G_i(t) + G_i^{(n)}(t+\Delta t)\right], \qquad (28)$$

$$B_i^{(n+1)}(t+\Delta t) = B_i(t) + \frac{\Delta t}{2}\left[G_i'(t) + G_i'^{(n)}(t+\Delta t)\right]. \qquad (29)$$

$$i = 2,4,\ldots 20, \qquad n = 1,2,\ldots.$$

Estimates at time $t + \Delta t$ are indicated by the superscript n while final estimates of quantities at time t are not superscripted. Initial estimates for $G_i^{(1)}(t+\Delta t)$ and $G_i'^{(1)}(t+\Delta t)$ are

$$G_i^{(1)}(t+\Delta t) = G_i(t), \qquad (30)$$

$$G_i'^{(1)}(t+\Delta t) = G_i'(t). \qquad (31)$$

The iterative process is continued, recalculating C and D for each new value of the superscript, until

$$\left| A_i^{(n+1)}(t+\Delta t) - A_i^{(n)}(t+\Delta t) \right| < \tau, \qquad (32)$$

$$\left| B_i^{(n+1)}(t+\Delta t) - B_i^{(n)}(t+\Delta t) \right| < \tau. \qquad (33)$$

When the above conditions are fulfilled, the new prognostic values of A and B are then used to calculate corresponding values of C and D. The process is continued for the desired time interval.

The amplitude of the pressure wave and phase angle can then be calculated using the relationships,

$$z' = R_z(\cos kx - S_z), \qquad (34)$$

$$R_z = \sqrt{A^2 + B^2}, \tag{35}$$

$$\tan \delta_z = A/B. \tag{36}$$

The model was programmed for solution by the CDC 1604 computer of the U. S. Naval Postgraduate School. The time step, Δt, was taken as 30 minutes, and the tolerance, τ, was 1 cm. Solutions for the amplitude and phase angle were obtained for every 6 hours up to 48 hours.

The heating function was introduced in the layers below 500 mb as a function of pressure in a manner suggested by Haltiner [2]. For this study, Q_1 was set equal to zero and

$$Q_2 = q_2 \left(\frac{p - p_{500}}{p_{500}}\right)^2. \tag{37}$$

In (37), q_2 represents the amount of heating being considered in joules/gr sec, p is the particular pressure level under consideration below 500 mb, and p_{500} is the 500-mb pressure. For the purpose of this investigation, q_2 was taken as 4×10^{-4} joules/gr sec which is approximately equivalent to heating of 400 langleys/day. Haltiner and Wang [3] propose that the exchange of heat between an air mass and underlying surface may be in excess of 800 langleys/day. However, it is felt that the 800+ figure represents an extreme, and that the value of 400 langleys/day is more representative.

The model is such that the heating function is constant in time and space for a given problem, while the phase angle and amplitude of the pressure wave are set initially and then allowed to develop.

Various permutations of the model were tested with different phase angles for the heating function, and with different wave lengths.

In all cases, σ was set equal to $.5 \times 10^{-4}$ cgs units, while β was equal to 1.6×10^{-13} cm^{-1} sec^{-1}. The wave lengths considered were 2000, 6000, and 10000 kilometers.

4. Results.

The results are expressed as a comparison between a no heat case and heating introduced with various phase angles.

a. The first model studied had linearized vertical shear with u_0 = 40 m/sec and $u_i = u_0\left(1 - \frac{p_i}{p_{1000}}\right)$, i = 50, 100...1000. The initial value of B at all levels was 97.4 meters and A at all levels was zero. The phase angle of the pressure wave was therefore zero at all levels.

With the initial input of heat in phase with the pressure wave, the development at the end of a 24-hr period in the lower layers was considerable for all wavelengths, (figure 2). However, in the layer 850-700 mb, a decrease in amplitude appears for the very long wave, 10000 km. The long wave, 6000 km, showed a similar pattern of development with a minimum of development in the same layer, 850-700 mb.

The movement of the pressure wave, as deduced from the phase angle, shows that the heating effect caused an increased movement of the long waves in the lower layers, (figure 3). Without heating, the very long wave retrogressed slowly at all levels throughout the period. For the initial 6-hour period with heating, it retrogressed slowly at all levels, then quite rapidly in the lower levels. As seen in figure 3, at the end of the 24-hr period, the retrogression in the upper levels is less than without heating, while in the lower levels it is considerably more. In 24 hours, the long wave progressed approximately one-quarter wavelength without heating. With heating, it retrogressed initially in the upper layers, while progressing in the lower. After 14 hours it progressed at all levels, so that after 24 hours, the net effect is progression. The short wave progressed over three-quarters of a wavelength without heating

at all levels, and slightly less with heating.

Choosing the 500-mb level as representative of the upper levels, a gradual increase in amplitude with time and heating was noted for all wavelengths, (figure 4).

The same model with the heating function initially 180 degrees out of phase with the pressure wave, showed that at the end of 24 hours, the two waves increased in amplitude below 750 mb, while all wavelengths increased below 900 mb, (figure 5). The 10000-km wave was the only one, when compared to the no heat case, which showed a larger amplitude at all levels. The 6000-km wave exhibited a marked decrease at all upper levels, while the short wave decreased slightly.

The very long wave retrogressed in all but the lowest layers. The short wave increased its progressive movement to approximately one wavelength, while the long wave decreased its movement, progressing slowly in the lower layers, and retrogressing in the upper layers, (figure 6).

A look at figure 7 for the development at 500-mb clarifies the case of the very long wave. It too decreased in amplitude until after approximately 18 hours had elapsed. This was true for all other levels.

For initial phase angles of the heating function of 90 and 270 degrees, the same marked increase in amplitude in the lower levels is evident, (figures 8 and 9). In the upper levels, for an initial angle of 90 degrees, the short wave decreased nearly uniformly, the long waves increased. For an initial angle of 270 degrees, the opposite appeared.

b. A second variation of the basic model included a linear vertical shear to 500 mb, and then a parabolic variation of the zonal wind to the top of the atmosphere. In this case, u_{500} equaled 20 m/sec, and u_{250} was 30 m/sec. A further modification was to allow for tilt of

the pressure wave by varying the phase angle in accordance with the relationship, phase angle equals $-\pi/2 \left(\frac{P_i}{P_{1000}}\right)^3$, $i = 0, 50, \ldots 1000$.

In all cases, this model showed extreme development below 900 mb for all wavelengths, regardless of the initial heating angle.

When the heating phase angle was zero, the 10000-km wave developed very slightly at upper levels, and decreased in the layer 650-800 mb, (figure 10). The 6000-km wave developed well above 700 mb, but with a minimum of development at 800 mb. The short wave evinced a nearly uniform increase in development at all levels above 800 mb.

For heating with an initial 180-degree phase angle, the 2000-km wave showed slight additional development above 700 mb except for a slight decrease in the layer 300-200 mb, and the 10000-km case showed increased development throughout, (figure 11). Again, an examination of the 500-mb level reveals that the very long wave did decrease in amplitude until beyond 12 hours, (figure 12).

A 270-degree heating phase angle produced increased amplification for all levels for the short wave, while both long waves decreased above 800 mb, (figure 13).

A 90-degree heating phase angle resulted in an increased amplitude of the 6000-km wave at all levels, (figure 14). The 10000-km wave showed a decreased amplitude from 900-800 mb, and increased above 800 mb. The short wave had decreased development at all levels above 900 mb.

c. A number of other cases were studied, however, the results were comparable to those reported, and therefore are not shown.

5. Conclusions.

The restrictions imposed upon the basic model lead to certain meteorological improbabilities, i.e., excessive speed of movement in certain cases and over amplification after twenty-four hours. However, it is felt that for short time periods, the relative development in the layers above 900 mb is plausible even on a quantitative basis.

BIBLIOGRAPHY

1. Rosenthal, S. L., 1964: Comparison of analytical and numerical solutions to an initial value problem defined by a linearized, quasi-geostrophic model, Monthly Weather Review, 92(12), 579-587, December, 1964.

2. Haltiner, G. L., 1965: Unpublished manuscript, Department of Meteorology, U. S. Naval Postgraduate School, Monterey, California.

3. Haltiner, G. L., and Yeh-chun Wang, 1959: Numerical prognosis including non-adiabatic warming, J. of Meteor., 17(2), 207-213, April, 1960.

APPENDIX I

Figures 2 through 14 referred to in text are included here for easy reference.

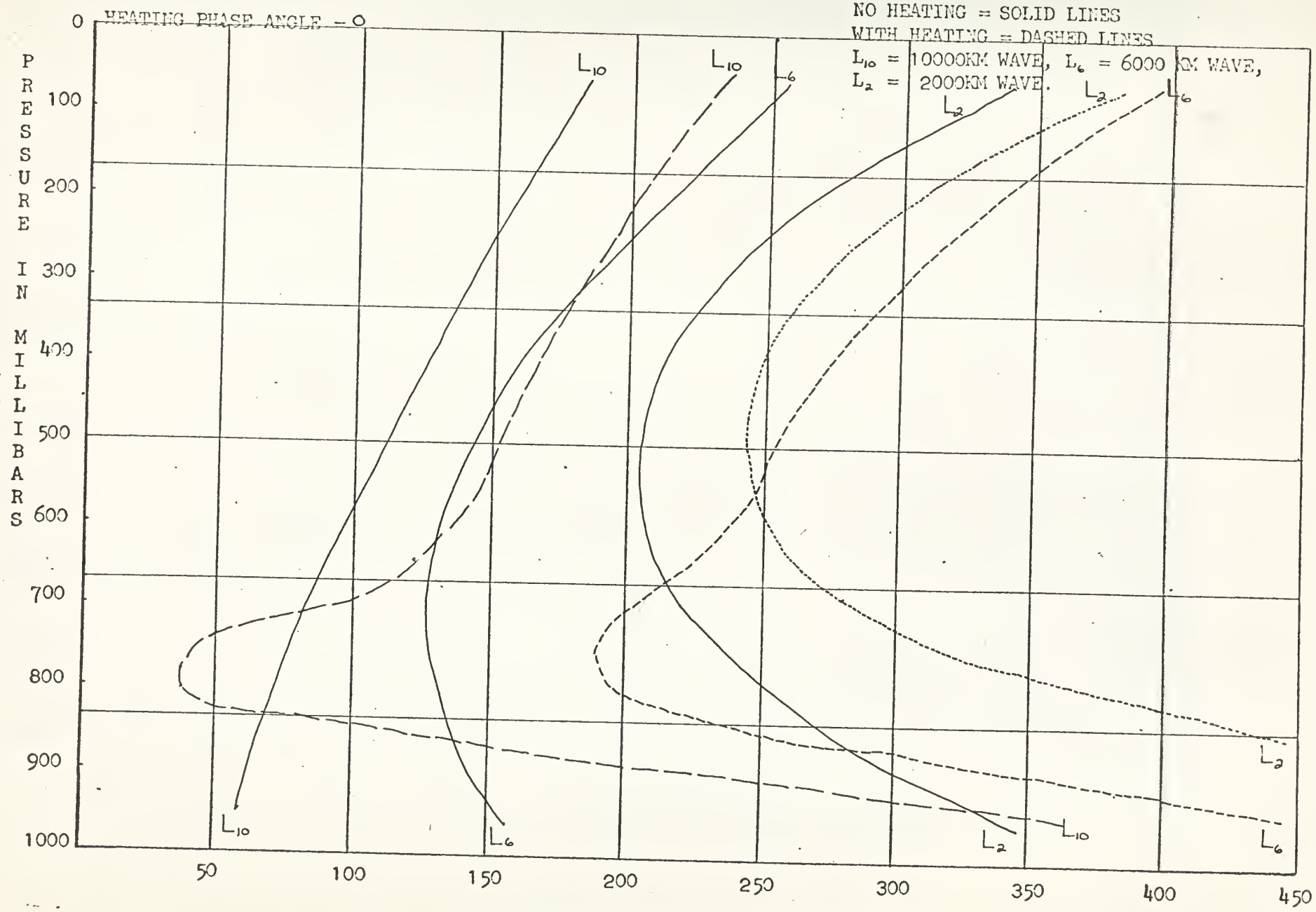

AMPLITUDE IN METERS AT 24 HOURS

FIGURE 2

A-1

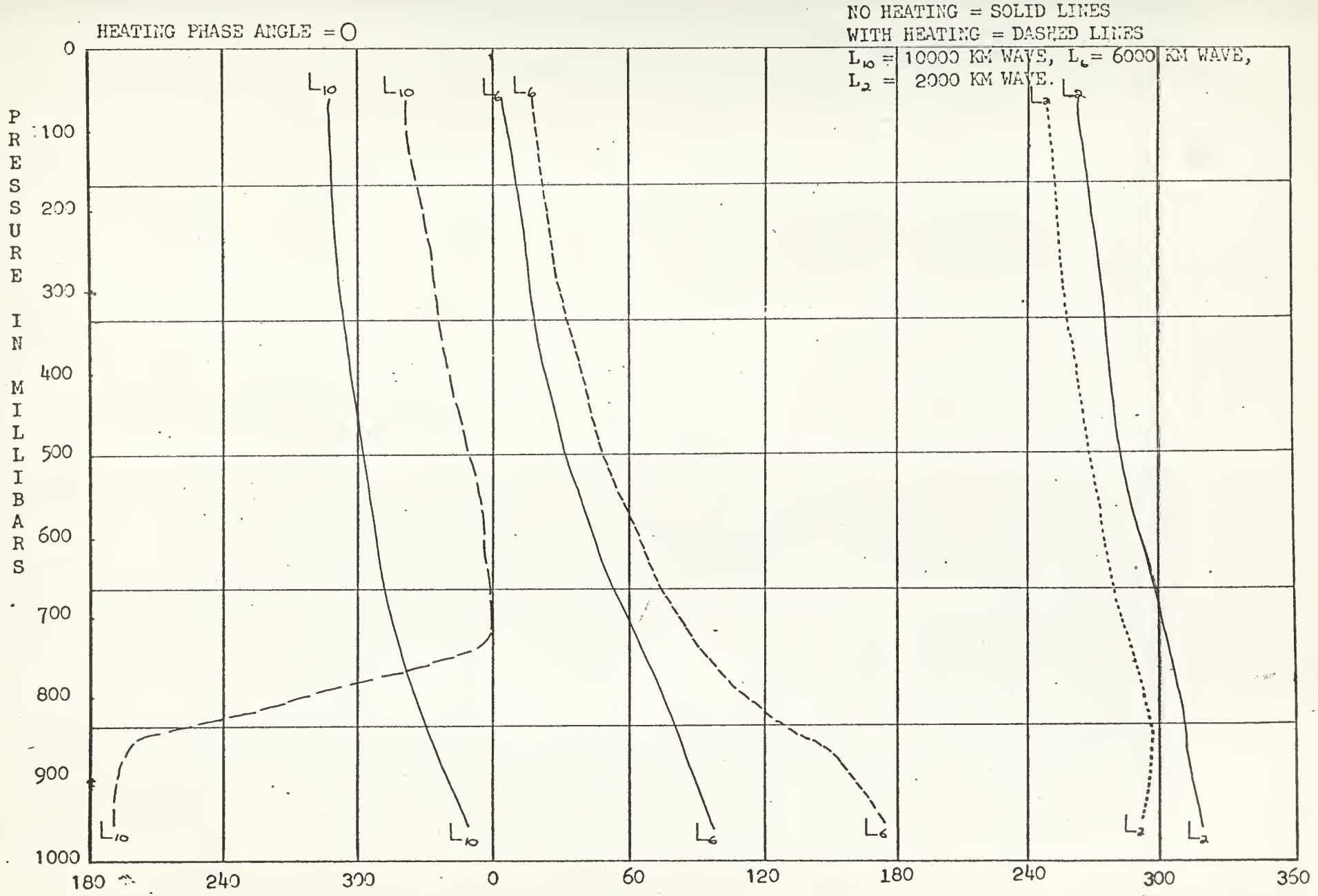
HEATING PHASE ANGLE = 0
NO HEATING = SOLID LINES
WITH HEATING = DASHED LINES
L_{10} = 10000 KM WAVE, L_6 = 6000 KM WAVE,
L_2 = 2000 KM WAVE.
PRESSURE IN MILLIBARS
0
100
200
300
400
500
600
700
800
900
1000
180
240
300
0
60
120
180
240
300
360
PHASE ANGLE IN DEGREES AT 24 HOURS

FIGURE 3

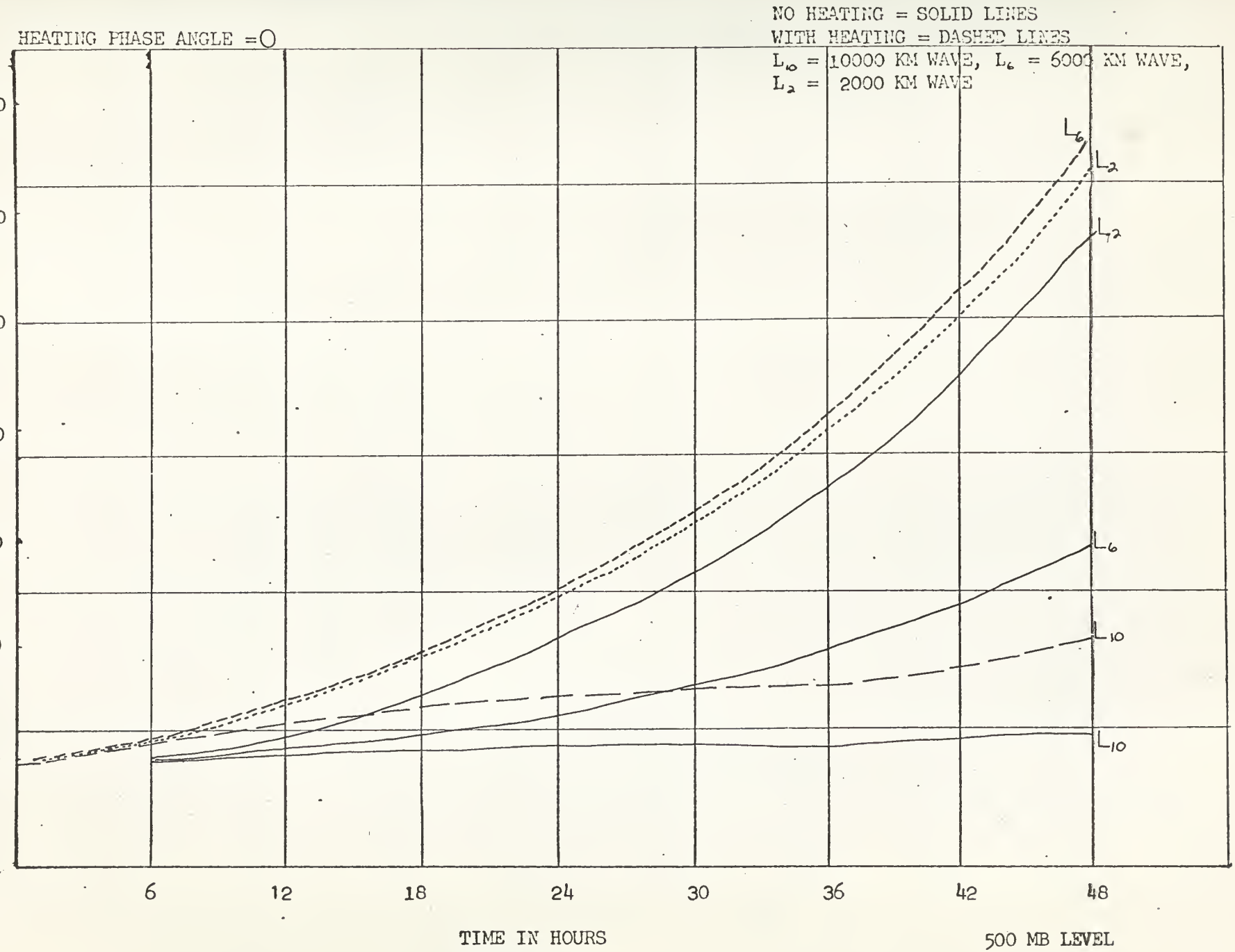
HEATING PHASE ANGLE =0
NO HEATING = SOLID LINES
WITH HEATING = DASHED LINES
L_{10} = 10000 KM WAVE, L_6 = 6000 KM WAVE,
L_2 = 2000 KM WAVE
AMPLITUDE IN METERS
100
200
300
400
500
600
700
6
12
18
24
30
36
42
48
L_6
L_2
L_2
L_6
L_{10}
L_{10}
TIME IN HOURS
500 MB LEVEL

FIGURE 4

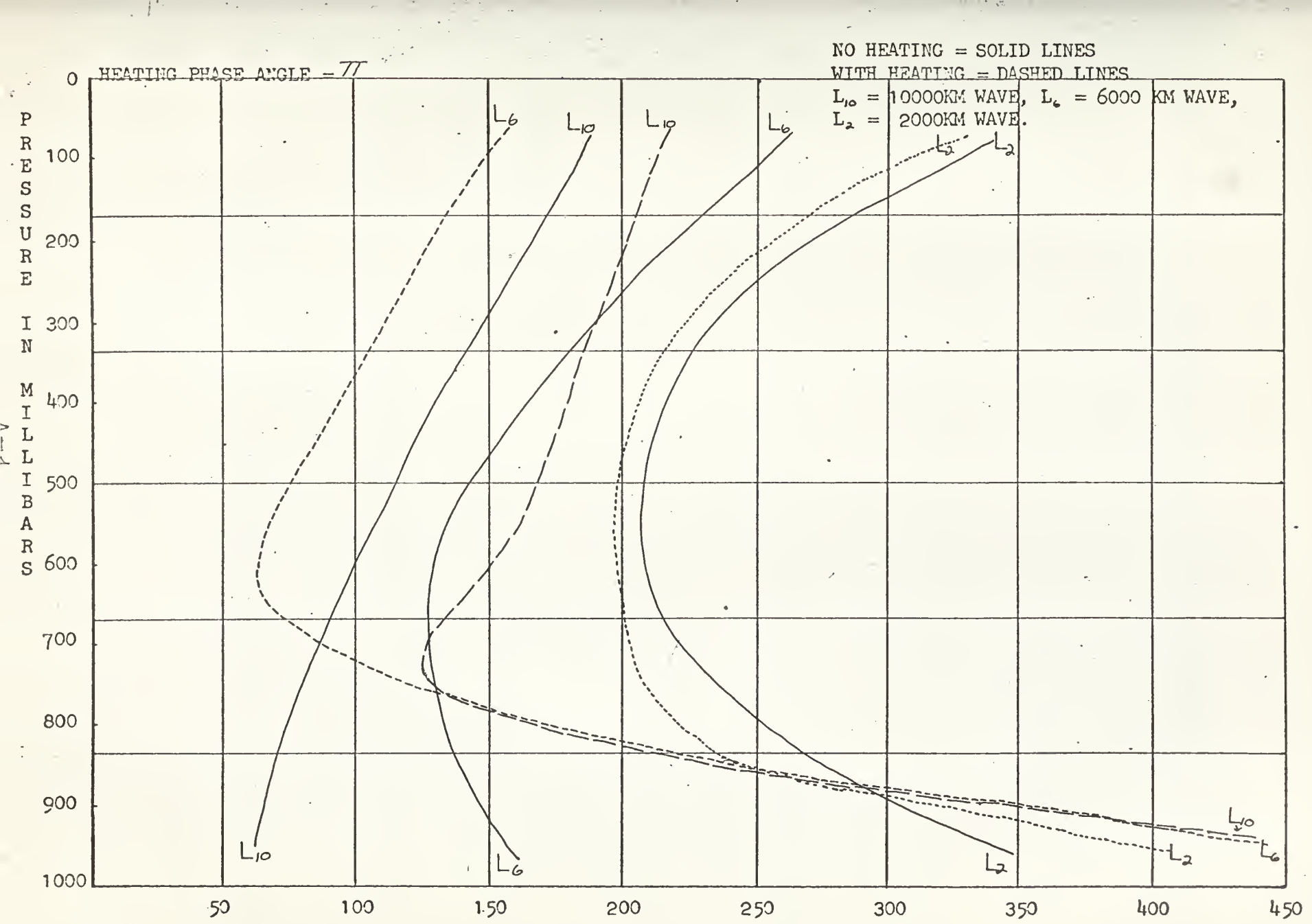

AMPLITUDE IN METERS AT 24 HOURS

FIGURE 5

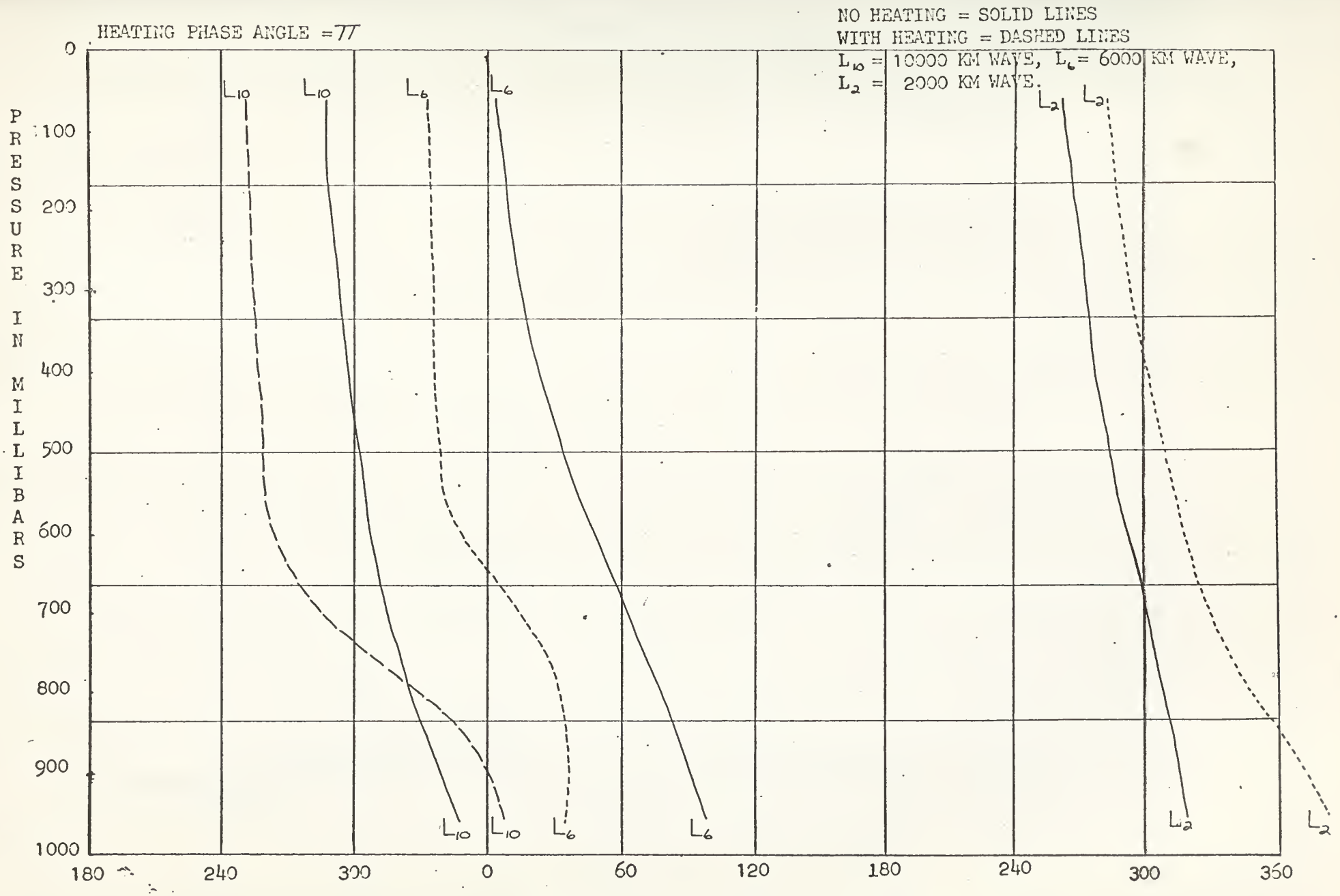
HEATING PHASE ANGLE = 77
NO HEATING = SOLID LINES
WITH HEATING = DASHED LINES
L_{10} = 10000 KM WAVE, L_6 = 6000 KM WAVE,
L_2 = 2000 KM WAVE.
PRESSURE IN MILLIBARS
0
100
200
300
400
500
600
700
800
900
1000
180
240
300
0
60
120
180
240
300
360
L_{10}
L_6
L_2
PHASE ANGLE IN DEGREES AT 24 HOURS

FIGURE 6

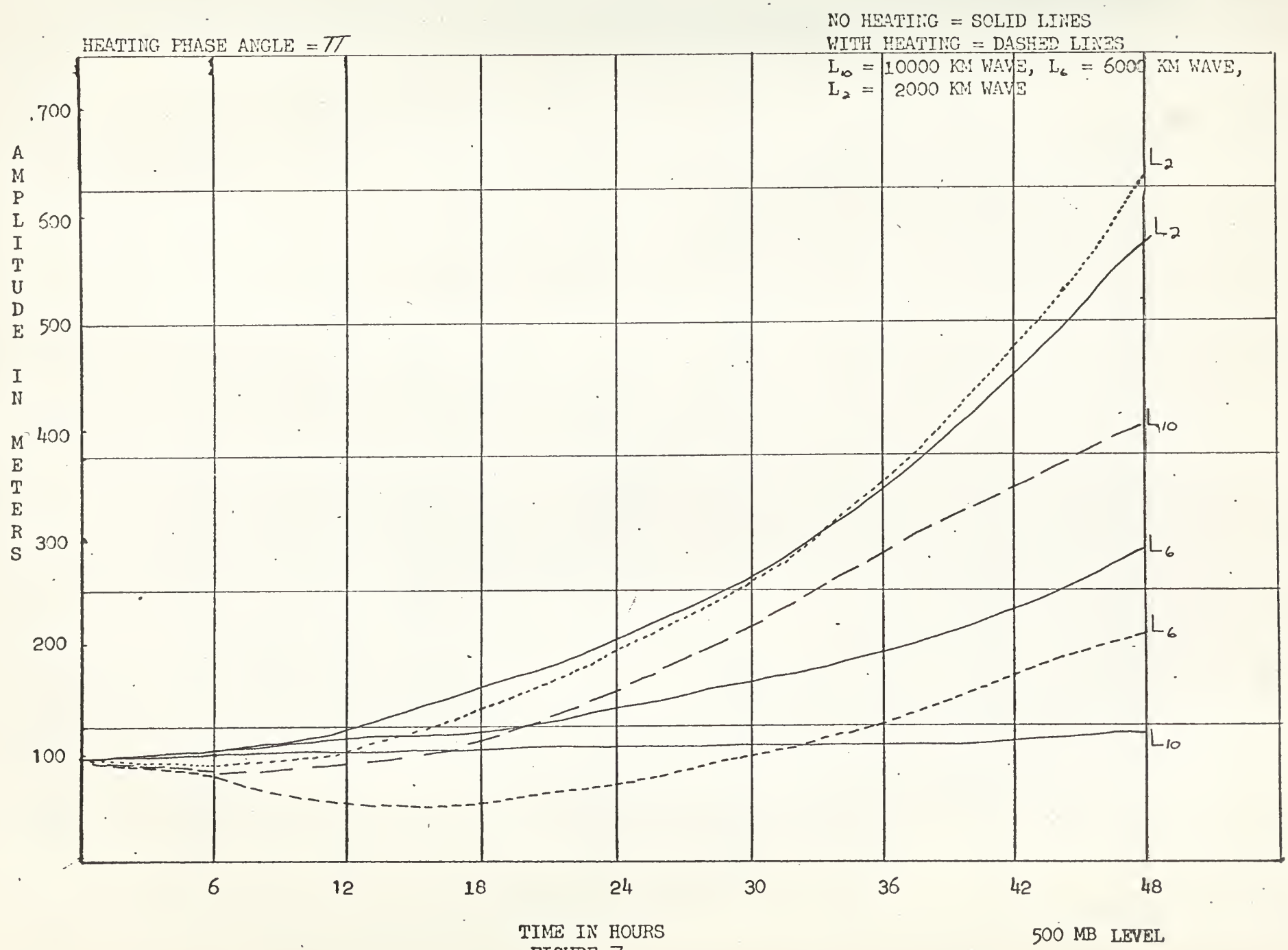

TIME IN HOURS

500 MB LEVEL

FIGURE 7

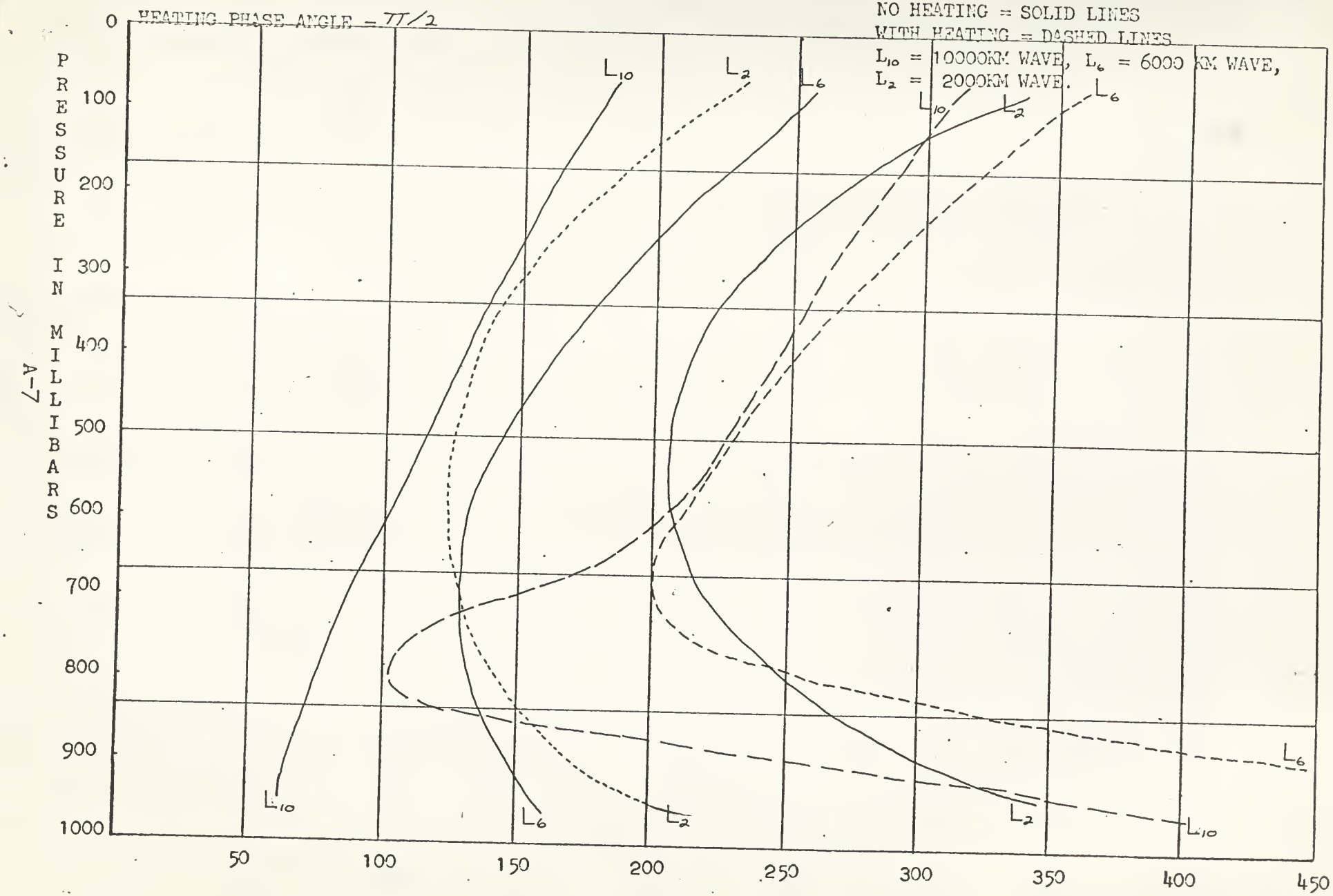

AMPLITUDE IN METERS AT 24 HOURS

FIGURE 8

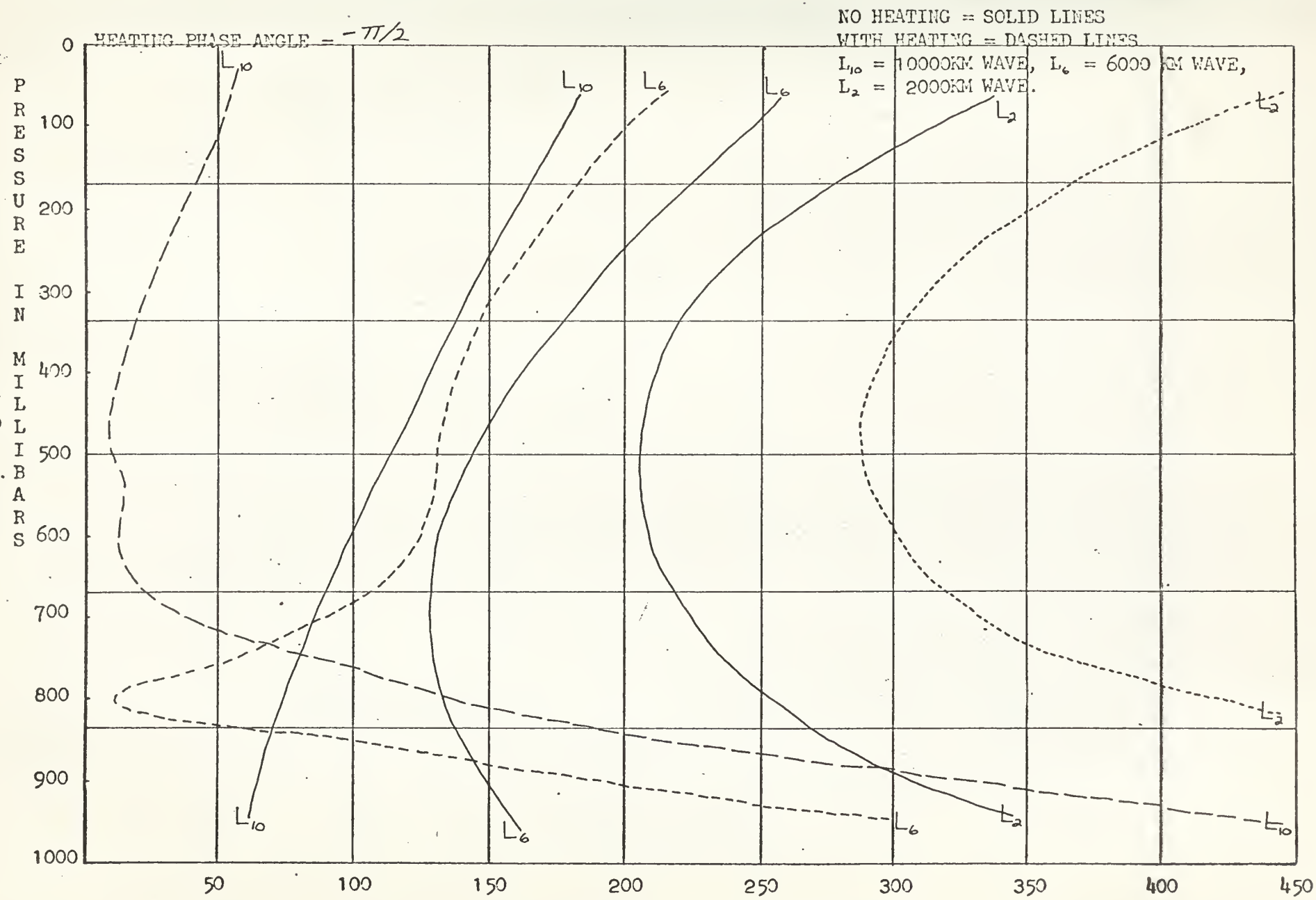
HEATING PHASE ANGLE = $-\pi/2$
NO HEATING = SOLID LINES
WITH HEATING = DASHED LINES
L_{10} = 10000KM WAVE, L_6 = 6000 KM WAVE,
L_2 = 2000KM WAVE.
PRESSURE IN MILLIBARS
0
100
200
300
400
500
600
700
800
900
1000
50
100
150
200
250
300
350
400
450
AMPLITUDE IN METERS AT 24 HOURS

FIGURE 9

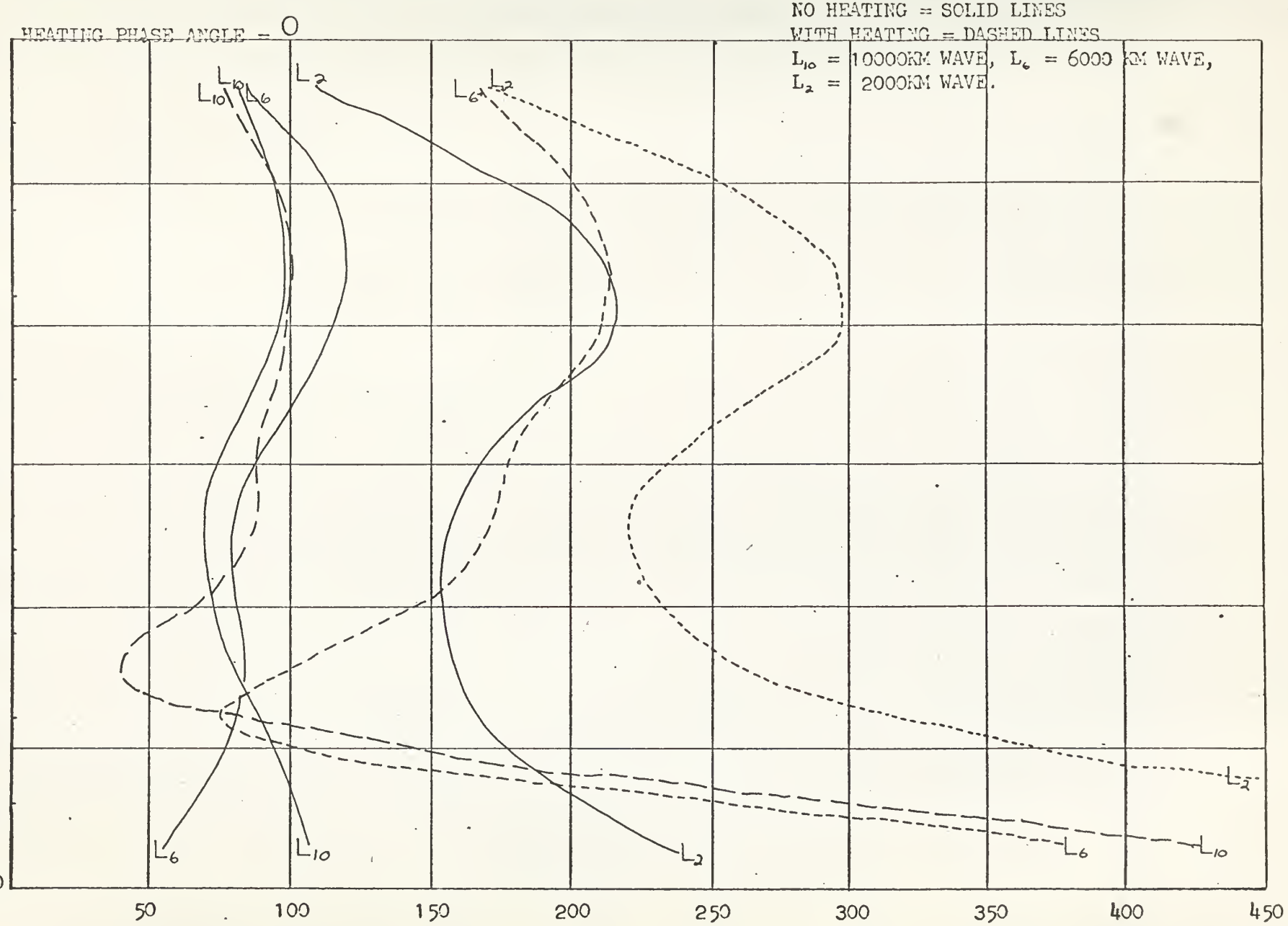

AMPLITUDE IN METERS AT 24 HOURS

FIGURE 10

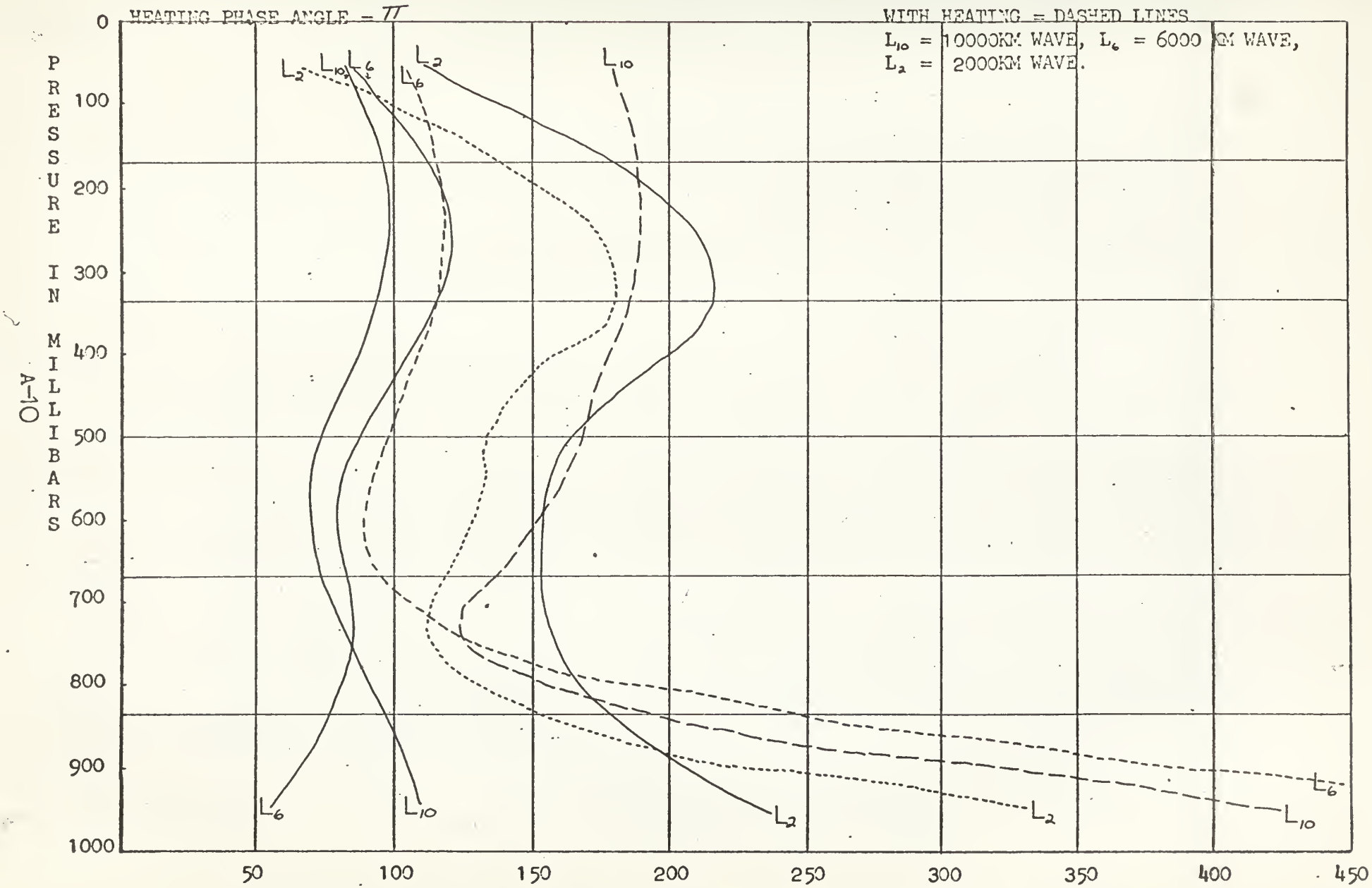

AMPLITUDE IN METERS AT 24 HOURS

FIGURE 11

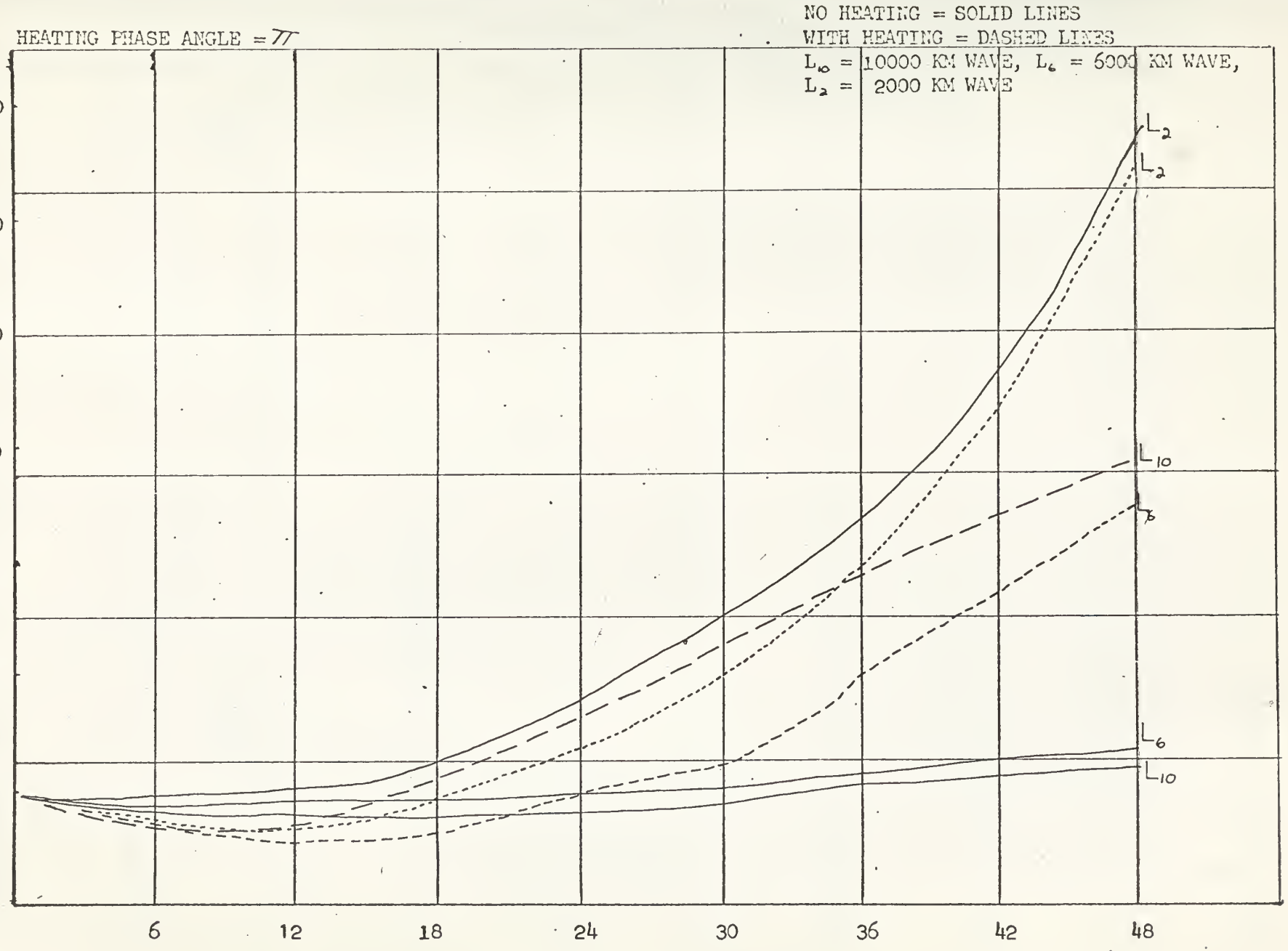

TIME IN HOURS

FIGURE 12

500 MB LEVEL

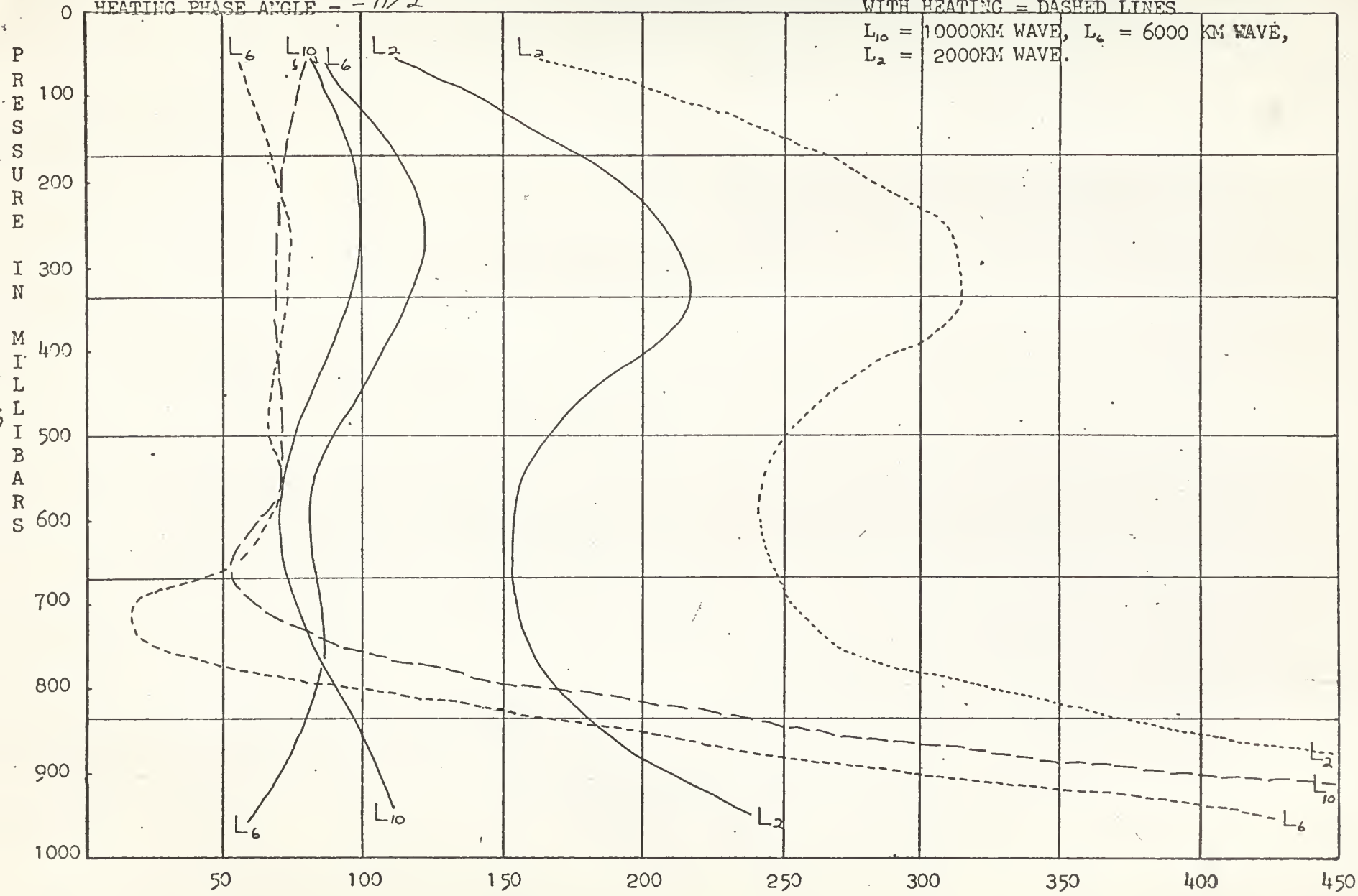

AMPLITUDE IN METERS AT 24 HOURS

FIGURE 13

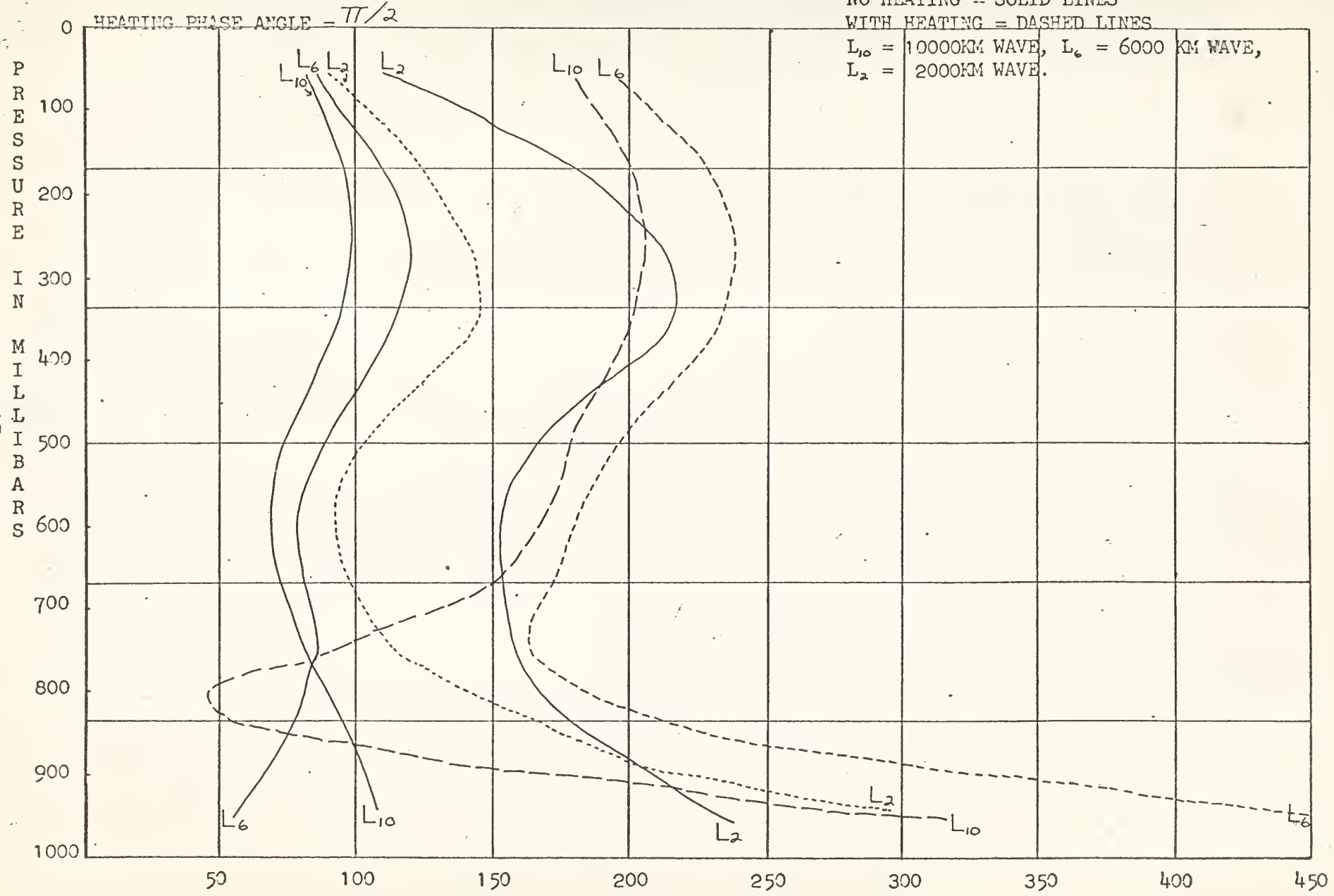

AMPLITUDE IN METERS AT 24 HOURS

FIGURE 14